DF-751
[1-6]

RESEARCH ARTICLE Agricultural Science Digest

# Nephrotoxicity of Iron Oxide Nanoparticles in Male Mice

Rawa Faris Hussein Al-Saeedi[1], Raghad Khalid Mwafaq[1], Noor Adel Jasim[2], Zina F.H. Al-Obaidi[3], Ahmed Flayyih Hasan[4,5], Hany M. El-Wahsh[6]

10.18805/ag.DF-751

## ABSTRACT

**Background:** The current study was conducted at Al-Nahrain University's Biotechnology Research Center. This study's objectives were to synthesize and characterize iron oxide nanoparticles ($Fe_2O_3$-NPs) and investigate the effects of varying concentrations on lipid peroxidation, the antioxidant defense system, biochemical parameters and kidney histology in male mice.

**Methods:** Twenty male Albinos Mice weighing between 25 and 30 g were utilized. The mice were split up into four groups of ten. Group II, Group III and Group IV received oral treatment with Tin oxide NPs at doses of 10, 25 and 50 mg/kg BW/day for four weeks, whereas the first group served as a control. Blood and kidney samples were taken for the examination of various parameters at the conclusion of the experiment.

**Result:** Creatinine and urea levels dramatically rose following treatment with iron oxide nanoparticles ($Fe_2O_3$-NPs) at varying doses. Treatment with iron oxide nanoparticles ($Fe_2O_3$-NPs) at varying concentrations resulted in a significant decrease in the activities of AST, ALT and ALP in mouse kidney homogenates, as well as a significant increase in lactate dehydrogenase (LDH). Histopathological changes were noted, confirming the biochemical perturbations caused by iron oxide nanoparticles ($Fe_2O_3$-NPs) at varying concentrations in mice kidney.

**Key words:** $Fe_2O_3$-NPs, Kidney histopathology, Liver, Mice, SOD, TBARS, Urea.

## INTRODUCTION

Nanotechnology is growing quickly. The growing use of nanotechnology goods, particularly in biomedical applications, has sparked worries about the possibility of unanticipated negative health consequences after exposure. Comprehending the toxicological profiles of engineered nanomaterials is essential to guaranteeing their safety for use and responsible development, which maximizes advantages while minimizing hazards. However, the creation of toxicity data is not keeping pace with the research and manufacturing of artificial nanomaterials (Dhakshinamoorthy *et al.,* 2017; Di Bona *et al.,* 2014; Zhang *et al.,* 2017; Yaseen *et al.,* 2025; M Obaid *et al.,* 2025). These organizations have published official documents addressing the need for focused research on suitable methodological tests for determining the toxicity of manmade nanomaterials (Yang *et al.,* 2015; Radu *et al.,* 2015; Yaseen *et al.,* 2024). Iron oxide nanoparticles (IONs) possess significant promise for a range of biological and biomedical uses, including tissue engineering, targeted drug or gene delivery, magnetic resonance imaging (MRI) contrast enhancement, biological fluid detoxification, cancer treatment-induced hyperthermia, cell labeling, cell sorting and immunoassay (Ying *et al.,* 2022). Few toxicological investigations have recently documented the changes in IOMNs' tissue distribution, toxicokinetic characteristics and gene expression in mice or rats following different exposure routes (Kolosnjaj-Tabi *et al.,* 2015; Obaid *et al.,* 2020). The manufacturing process, surface features and particle size are all strongly correlated with the hydrodynamic size of IONs, which in turn influences the magnetic and biological properties, biodistribution, toxicokinetics, elimination and toxicity (De Barros *et al.,* 2014; Obaid *et al.,* 2020). The location of $Fe_3O_3$ MNPs in the vital organ tissues and their *in vivo* metabolic processes inside the body are still unclear, nevertheless. We used imprinting control region (ICR) mice as an experimental paradigm to synthesize $Fe_3O_3$ MNPs by chemical coprecipitation. Given the application viewpoint of $Fe_3O_3$ NMPs, the mice were administered the NMPs intragastrically. Atomic absorption spectrophotometry was used to assess the amounts of $Fe_3O_4$ MNPs in various organs and tissues at certain time points (Sharma *et al.,* 2018; Salimi *et al.,* 2020; Kareem *et al.,* 2023).

[1]Collage of Science, AL Karakh University of Sciences, Baghdad, Iraq.
[2]Department of Forensic Evideetnce,College of Science, Al-Nahrain University, Baghdad, 10072, Iraq.
[3]Department of Medical and Molecular Biotechnology, College of Biotechnology, Al-Nahrain University, Baghdad, Iraq.
[4]Biotechnology Research Center, Al-Nahrain University, Baghdad, Iraq.
[5]Department of Biology, Al-Farabi University College, Baghdad, Iraq.
[6]Department of Marine Biology, Faculty of Marine Sciences, King Abdulaziz University, Saudi Arabia.

**Corresponding Author:** Ahmed Flayyih Hasan, Biotechnology Research Center, Al-Nahrain University, Baghdad, Iraq.
Email: ahmed_flayyih@nahrainuniv.edu.iq
ORCID: 0009-0007-9208-5046

**How to cite this article:** Al-Saeedi, R.F.H., Mwafaq, R.K., Jasim, N.A., Al-Obaidi, Z.F.H., Hasan, A.F. and El-Wahsh, H.M. (2025). Nephrotoxicity of Iron Oxide Nanoparticles in Male Mice. Agricultural Science Digest. 1-6. doi: 10.18805/ag.DF-751.

**Submitted:** 28-04-2025 **Accepted:** 03-07-2025 **Online:** 16-07-2025

## MATERIALS AND METHODS

### Chemicals

The following agents were procured from Sigma-Aldrich (St. Louis, USA).

### Animals and experimental design

The experimental protocol was approved by the Local Ethics Committee and Animals Research and twenty male Albino mice weighing 25-30 g were acquired from the Al-Nahrain University animal house.

**GP1:** Control rats were orally for a period of 4 weeks.

**GP2:** $Fe_2O_3$-NPs were administered orally to mice for four weeks at a rate of 50 mg/kg BW/day.

**GP3:** Mice were treated orally with $Fe_2O_3$-NPs at a dose of 25 mg/kg BW/day for a period of 4 weeks.

**GP4:** Mice were treated orally with $Fe_2O_3$-NPs at a dose of 10 mg/kg BW/day for a period of 4 weeks.

Mice were fasted overnight, put to sleep and then dissected at the conclusion of the experiment. For biochemical tests, blood samples were extracted from the aorta and placed in glass tubes devoid of anticoagulants. Each rat's abdominal cavity was opened and the kidney and liver were removed. Histological and biochemical analyses were performed on these tissues.

### Blood and serum samples

Each rat's aorta was used to draw blood, which was then inside glass tubes that have not been heparinized. Centrifugation was used for 15 minutes at 3000 rpm to separate the serum. Before being examined, the collected serum was kept at -18°C.

### Tissue samples

The kidneys of the scarified mice were immediately removed and cleansed with cold saline. After that, they were weighed and cleaned using a cooled saline solution at a concentration of 0.9%. The tissues were chopped and homogenized (10% w/v) in a Potter-Elvehjem-type homogenizer with 1.15% KCl in ice-cold sodium phosphate buffer (0.01 M, pH 7.4). For 20 minutes at 4°C, the homogenates were centrifuged at 10,000 xg. The various enzyme activity, free radicals and biochemical parameters were analyzed using the resulting supernatants.

### Determination of thiobarbituric acid-reactive substances content

The technique was used to quantify thiobarbituric acid-reactive compounds (TBARS) in liver and kidney homogenate of Ohkawa *et al.* (1979).

### Determination of hydrogen peroxideand educed glutathione content concentration

In an ice bath, 100 mg of sample tissue was extracted using 5 ml of TCA (0.1%, w/v) and it was centrifuged for 15 minutes at 12,000 × g in order to determine the hydrogen peroxide ($H_2O_2$) concentration (Velikova *et al.,* 2000; Altemeemi *et al.,* 2021).

### Determination of urea and creatinine concentration

A commercial kit provided by Diamond, Egypt, was used to measure the levels of creatinine and urea in the serum. The Patton and Crouch technique was used to estimate urea (1977).

### Histopathological examination

Hematoxylin and eosin stain (Bancroft and Stevens, 1990) was used to prepare serial paraffin slices of kidneys that had been preserved in Bouin's solution for histological analysis. These sections were then seen under a light microscope According to (Al-Khuzaay *et al.,* 2024; Yahya *et al.,* 2024; Hameed *et al.,* 2025; Abd El-Rahmana *et al.,* 2024).

### Ethical approval

This research was initiated after receiving the consent of the Medical Research Ethics Committee, Al-Nahrain University/Biotechnology Research Center.

### Statistical analysis

Each measurement was performed twice in different experiments for each treatment. The data were expressed as mean ± standard error (SE). SPSS 17 was utilized to perform the statistical analyses, which included one-way analysis of variance (ANOVA).

## RESULTS AND DISCUSSION

### Effect of different concentrations of Iron oxide nanoparticles in mice kidney

According to the data in Table 1, the kidney homogenate of male rats treated with varying concentrations of iron oxide nanoparticles demonstrated a concentration-dependent

**Table 1:** Effect of different concentrations of Iron oxide nanoparticles in mice kidney.

| Parameters | Experimental groups | | | |
|---|---|---|---|---|
| | Cont. | $Fe_2O_3$-NPs 50 mg/kg BW/day | $Fe_2O_3$-NPs 25 mg/kg BW/day | $Fe_2O_3$-NPs 10 mg/kg BW/day |
| TBARS (nmol/g tissue) | 21.44±0.66$^{d}$ | 28.22±0.733$^{c}$ | 31.80±2.22$^{b}$ | 36.70±0.801$^{ab}$ |
| $H_2O_2$ (µmol/g tissue) | 41.60±2.70$^{d}$ | 55.01±2.39$^{c}$ | 61.10±2.77$^{bc}$ | 68.11±4.22$^{ab}$ |
| GSH (mmol/mg protein) | 3.44±0.011$^{a}$ | 2.14±0.055$^{b}$ | 1.80±0.055$^{b}$ | 1.70±0.044$^{c}$ |

significant increase in hydrogen peroxide ($H_2O_2$) and thiobarbituric acid reactive substances (TBARS) when compared to the control and other iron oxide nanoparticle groups. However, compared to the control, the reduced glutathione level (GSH) was much lower.

**Effect of different concentrations of Iron oxide nanoparticles in mice kidney**

Table 2 displays information on the activity of the kidney antioxidant SOD, CAT, GPx, GR and GST enzymes. In comparison to the control group, the activity of antioxidant enzymes was significantly ($P<0.05$) reduced in a number of rat groups treated with iron oxide nanoparticles.

**Effect of different concentrations of Iron oxide nanoparticles in mice kidney**

Iron oxide nanoparticles at varying concentrations dramatically reduced the protein content of the rat kidney while considerably increasing serum urea and creatinine, as seen in Table 3, as compared to the control group.

**Kidney histopathology**

Fig 1 shows the morphological and histological changes in kidney tissues in all different study groups. The results showed the following:. G1: The photomicrograph of the kidney sections stained with H and E in the control mice showed normal histological characteristics of the renal tubules (Tb) and glomruli (g) in the cortical portion.G2: A photomicrograph of the kidney sections stained with H and E after receiving 50 mg/kg BW/day of $Fe_2O_3$-NPs revealed mild to severe vascular degeneration in the renal tubule lining epithelial cells.G3: Photomicrographs of the kidney sections stained with H and E after receiving a dose of $Fe_2O_3$-NPs at a rate of 25 mg/kg BW/day revealed pyknotic nuclei, considerable localized necrosis, and an increased incidence of vacuolar degeneration.G4: A photomicrograph of the kidney sections stained with H and E after receiving a dosage of $Fe_2O_3$-NPs at a rate of 10 mg/kg BW/day showed pyknotic nuclei, significant localized necrosis, and an increased incidence of vacuolar degeneration.

These enzymes function independently and are kept up properly in concert and in concert to preserve the integrity and proper operation of tissues and cells under typical physiological settings. In the current work, rats fed $Fe_2O_3$-NPs showed elevated levels of TBARS and $H_2O_2$ and lower levels of antioxidants such GSH, indicating enhanced oxidative stress in kidney tissues (Ghaznavi *et al.,* 2022. The higher use of GSH to fight potassium free radicals or the binding of the -SH group to nanoparticles may be the cause of the drop in GSH levels. These results were in agreement with both ( Reddy *et al.,* 2017; Luo *et al.,* 2024; Abd El-Aziz *et al.,* 2024). In order to keep ROS at appropriate levels, An impressive array of defense mechanisms is provided by antioxidant enzymes. Even little variations (Jomova *et al.,* 2024). Because it catalyzes the conversion of superoxide radicals into $H_2O_2$, (Pereira *et al.,* 1994; Gusti *et al.,* 2021; Al-Maliki *et al.,* 2025). Together with glutathione peroxidase, the ubiquitous enzyme catalase is a key component of the antioxidant defense system and catalyzes the breakdown of $H_2O_2$ into $H_2O$. Mice given $Fe_2O_3$-NPs at varying dosages for three weeks in the current study demonstrated a considerable reduction in protein content and alkaline phosphatase (ALP) activity, but a rise in lactate dehydrogenase activity. Following kidney damage, these enzymes are released into the bloodstream, which

**Table 2:** Effect of different concentrations of Iron oxide nanoparticles in mice kidney.

| Parameters | Experimental groups | | | |
|---|---|---|---|---|
| | Cont. | $Fe_2O_3$-NPs 50 mg/kg BW/day | $Fe_2O_3$-NPs 25 mg/kg BW/day | $Fe_2O_3$-NPs 10 mg/kg BW/day |
| SOD (U/mg protein) | 59.66±3.22$^{a}$ | 51.77±2.44$^{b}$ | 44.33±3.66$^{c}$ | 41.17±2.31$^{cd}$ |
| CAT (μmol/hr/mg protein) | 60.11±2.33$^{a}$ | 48.11±3.22$^{b}$ | 43.33±2.11$^{c}$ | 39.22±0.77$^{d}$ |
| GPx (U/mg protein) | 27.66±0.88$^{a}$ | 23.04±0.732$^{b}$ | 20.21±0.55$^{c}$ | 17.22±0.45$^{cd}$ |

Means ± SE are used to express values; each treatment group has five members. ABCD significant differences were observed between mean values within a row that did not share a common superscript letter ($p<0.05$).

**Table 3:** Effect of different concentrations of Iron oxide nanoparticles in mice kidney.

| Parameters | Experimental groups | | | |
|---|---|---|---|---|
| | Cont. | Fe2O3-NPs 50 mg/kg BW/day | Fe2O3-NPs 25 mg/kg BW/day | Fe2O3-NPs 10 mg/kg BW/day |
| Urea (mg/dl) | 40.22±3.29$^{d}$ | 44.07±1.29$^{c}$ | 47.11±2.33$^{bc}$ | 50.06±4.22$^{ab}$ |
| Creatinine (mg/dl) | 0.633±0.011$^{d}$ | 0.766±0.012$^{c}$ | 0.790±0.033$^{bc}$ | 0.841±0.041$^{ab}$ |
| LDH (U/mg protein) | 879±40.70$^{d}$ | 933±19.11$^{c}$ | 1089±30.05$^{b}$ | 1148±41.08$^{ab}$ |
| ALP (U/mg protein) | 181±7.11$^{a}$ | 177±3.33$^{b}$ | 157±4.03$^{c}$ | 140±6.66$^{d}$ |
| Protein (mg/g tissue) | 70.66±3.50$^{a}$ | 61.05±4.06$^{b}$ | 55.41±3.33$^{b}$ | 45.11±3.45$^{c}$ |

Means ± SE are used to express values; each treatment group has five members. ABCD significant differences were observed between mean values within a row that did not share a common superscript letter ($p<0.05$).

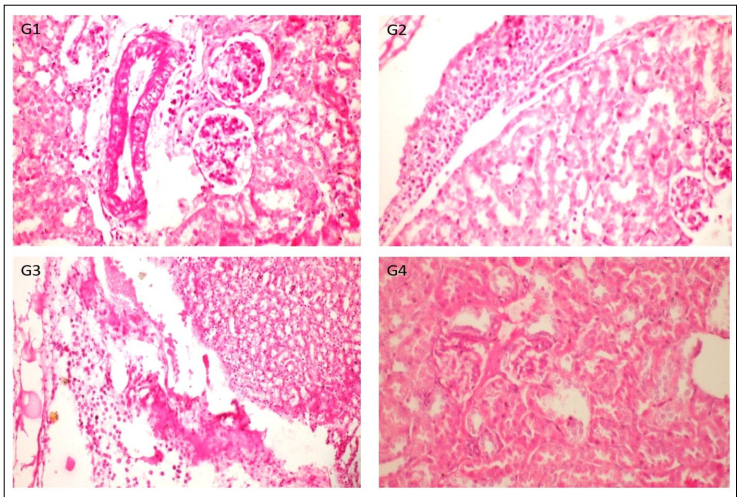


G1: Normal histological features of the glomruli (g) and renal tubules (Tb) in the cortical part were seen in the photomicrograph of the kidney sections stained with H andE in the control mice. G2: Following the treatment of 50 mg/kg BW/day of $Fe_2O_3$-NPs, a photomicrograph of the kidney sections stained with H and E showed mild to severe vascular degeneration in the renal tubule lining epithelial cells. G3: Following the administration of a dosage of $Fe_2O_3$-NPs at a rate of 25 mg/kg BW/day, the kidney sections' photomicrographs stained with H andE showed significant localized necrosis, pyknotic nuclei and an elevated incidence of vacuolar degeneration. G4: Following the administration of a dosage of $Fe_2O_3$-NPs at a rate of 10 mg/kg BW/day, a photomicrograph of the kidney sections stained with H andE revealed significant localized necrosis, pyknotic nuclei and an elevated incidence of vacuolar degeneration.

**Fig 1:** Hematoxylin and Eosin-stained photomicrographs of kidney slices in each group.

causes an increase in their activity in serum samples (Mishra *et al.,* 2017; Al-Maliki *et al.,* 2024). It's common knowledge that lipid peroxidation weakens cell membranes, allowing cytoplasmic enzymes to leak out (Bagchi *et al.,* 1995). Thus, liver, kidney and lung necrosis may be the cause of the lower activity of these enzymes in serum shown in our investigation (Wang *et al.,* 2010; Zedan *et al.,* 2023). Xinobiotics have been shown to alter the activities of several enzymes in various tissue organs. Normal histological structures of the glomruli and renal tubules in the cortical and medullary regions were found in the control rat group's kidney sections stained with hematoxylin and eosin. Bowman's capsule and proximal and distal convoluted tubules encircle the glomerulus, which is free of inflammatory alterations. A basic squamous epithelium is formed by cells in Bowman's capsule's outer or parietal layer. Because of their very diverse shapes, cells in the inner layer are invisible to histological routine staining. The glomerulei have an oval or circular form. The kidney segment showed modest to severe vascular degradation in the cortical zone of the renal tubule lining epithelial cells with pyknotic and karyolyzed nuclei following the injection of iron oxide nanoparticles. On the other hand, following the administration of iron oxide nanoparticles, kidney sections showed numerous abnormalities in the cortex and medulla renal structures, including the loss of the characteristic Malpighian corpuscles and the appearance of renal tubules with a wide lumen and degenerated epithelium, as well as pyknotic nuclei, increased incidence of vacuolar degeneration and noticeable congestion in the renal blood vessels (Fig 1). Numerous high-quality nanomaterials have surfaced as a result of the quick development of nanotechnology and because of their special biological characteristics, they are widely used in medicine, cosmetics, coatings, new materials, catalysts and many other fields to enhance existing products or create ones with new functions (Balas *et al.,* 2021; Saleh *et al.,* 2024). Exposure to nanomaterials is getting more likely, but the safety concern is also growing more acute. According to early toxicological research, nanoparticles may have a negative effect on both the environment and human health (Tate *et al.,* 2009; Ghiath *et al.,* 2025; Zedan *et al.,* 2022).

## CONCLUSION

Iron oxide nanoparticles (Fe2O3-NPs) clearly had significant negative effects on mice's kidneys in a dose-dependent manner. Biomarkers for the detrimental effects of iron oxide nanoparticles ($Fe_2O_3$-NPs) might include biochemical measures, lipid peroxidation estimation and enzymatic and non-enzymatic antioxidants.

## ACKNOWLEDGEMENT

No funding agency awarded a grant for this work.

### Conflict of interest

All authors declared that there is no conflict of interest.

## REFERENCES


Abd El-Aziz, Y.M., Alaryani, F.S., Aljahdali, N., Majrashi, K.A., Albaqami, N.M., Khattab, M.S. and Abu Almaaty, A.H. (2024). Impact of Punica granatum seeds extract (PSE) on renal and testicular tissues toxicity in mice exposed to iron oxide nanoparticles (IONPs). *Scientific Reports.* **14(1):** 26067.

Abd El-Rahmana, H.A., Hasanb, A.F., Alyasiric, T., El-Wahshd, H.M., Althubyanie, S.A., Basyonyf, M.A. and Mahmodf, D.H. (2024). Co-treatment with cranberry and vitamin-C mitigates reproductive toxicities induced by phenobarbital in male rats. *Cell Physiol Biochem.* **58:** 722-738.

Al-Khuzaay, H.M., Al-Juraisy, Y.H., Hasan, A.F. and Tousson, E. (2024). Antitumor activity of β-glucan isolated àrom date fruits on cancer cells *in vivo*. *Opera Medica et Physiologica.* **11(3):** 41-48.

Al-Maliki, N.S. and Zedan, Z.K. (2024). miRNA-126 as a biomarker for cancer stem cells: Role in chemotherapy resistance in Iraqi patients with acute myeloid leukemia. *Al-Rafidain Journal of Medical Sciences.* (ISSN 2789-3219). **6(1):** 195-199.

Al-Maliki, N.S., Jumaah, Y.H., Hameed, H.M., Khudhair, O.E., Hadid, M.A. and Hasan, A.F. (2025). Evaluation of miRNA-155 as a biomarker for cancer stem cells and its role in chemotherapy resistance in Iraqi patients with acute myeloid leukemia. *Opera Medica et Physiologica.* **12(1):** 30-37.

Altemeemi, A.S., Kadhim, N.K. and Nsaif, G.S. (2021). Changes in interleukins and follicle stimulating hormone in toxoplasmosis male patients. *Indian Journal of Forensic Medicine and Toxicology.* **15(1):** 803-807.

Bagchi, D., Bagchi, M., Hassoun, E.A. and Stohs, S.J. (1995). *In vitro* and *in vivo* generation of reactive oxygen species, DNA damage and lactate dehydrogenase leakage by selected pesticides. *Toxicology.* **104(1-3):** 129-140.

Balas, M., Popescu Din, I.M., Hermenean, A., Cinteza, L.O. and Dinischiotu, A. (2021). Exposure to iron oxide nanoparticles coated with phospholipid-based polymeric micelles induces renal transitory biochemical and histopathological changes in mice. *Materials.* **14(10):** 2605.

Bancroft, J.D., Stevens, A. (1990). Theory and practice of histological techniques. 3rd *ed. Edinburgh: Churchill Livingstone.*

De Barros, A.L.B., Chacko, A.M., Mikitsh, J.L., Al Zaki, A., Salavati, A., Saboury, B. and Alavi, A. (2014). Assessment of global cardiac uptake of radiolabeled iron oxide nanoparticles in apolipoprotein-E-deficient mice: Implications for imaging cardiovascular inflammation. *Molecular Imaging and Biology.* **16:** 330-339.

Dhakshinamoorthy, V., Manickam, V. and Perumal, E. (2017). Neuro-behavioural toxicity of iron oxide nanoparticles in mice. *Neurotoxicity Research.* **32:** 187-203.

Di Bona, K.R., Xu, Y., Ramirez, P.A., DeLaine, J., Parker, C., Bao, Y. and Rasco, J.F. (2014). Surface charge and dosage dependent potential developmental toxicity and biodistribution of iron oxide nanoparticles in pregnant CD-1 mice. *Reproductive Toxicology.* **50:** 36-42.

Ghaznavi, H., Hajinezhad, M.R., Shirvaliloo, M., Shahraki, S., Shahraki, K., Saravani, R. and Sargazi, S. (2022). Effects of folate-conjugated Fe2O3@ Au core-shell nanoparticles on oxidative stress markers, DNA damage and histopathological characteristics: evidence from *in vitro* and *in vivo* studies. *Medical Oncology.* **39(9):** 122.

Ghiath, Y., Mtashar, B.A., AL-Zuhairy, N.A.H.S., Hussein, M.S. and Hasan, A.F. (2025). Interplaying correlation of some genetic and inflammatory factors among patients with polycythemia vera. *Asian Journal of Dairy and Food Research.* 1-6. doi: 10.18805/ajdfr.DRF-492.

Gusti, A.M., Qusti, S.Y., Alshammari, E.M., Toraih, E.A.and Fawzy, M.S. (2021). Antioxidants-related superoxide dismutase (SOD), catalase (CAT), glutathione peroxidase (GPX), glutathione-S-transferase (GST) and nitric oxide synthase (NOS) gene variants analysis in an obese population: A preliminary case-control study. *Antioxidants.* **10(4):** 595.

Hameed, H.M., Razooki, Z.H. and Hasan, A.F. (2025). Therapeutic effect of essential oils (*Citrus sinensis*) against ehrlich ascites model induced renal toxicity in female mice. *Agricultural Science Digest.* **45(2):** 317-322. doi: 10.18805/ag.DF-632.

Jomova, K., Alomar, S.Y., Alwasel, S.H., Nepovimova, E., Kuca, K. and Valko, M. (2024). Several lines of antioxidant defense against oxidative stress: Antioxidant enzymes, nanomaterials with multiple enzyme-mimicking activities and low-molecular-weight antioxidants. *Archives of Toxicology.* **98(5):** 1323-1367.

Kareem Kadhim, N. and Hussein Zwamel, A. (2023). The GGC medium reduces the DNA fragmentation of human spermatozoa *via in vitro* activation. *Archives of Razi Institute.* **78(2):** 709-714.

Kolosnjaj-Tabi, J., Javed, Y., Lartigue, L., Volatron, J., Elgrabli, D., Marangon, I. and Gazeau, F. (2015). The one year fate of iron oxide coated gold nanoparticles in mice. *ACS Nano.* **9(8):** 7925-7939.

Lowry, O.H., Rosebrough, N.J., Farr, A.L., Randall, R.J. (1951). Protein measurement with Folin phenol reagent. *J. Biol Chem.* **193:** 265-275.

Luo, C., Li, X., Yan, H., Guo, Q., Liu, J. and Li, Y. (2024). Iron oxide nanoparticles induce ferroptosis under mild oxidative stress *in vitro*. *Scientific Reports.* **14(1):** 31383.

M Obaid, R., Tareq Yaseen, F., Kareem Kadhim, N., Hameed Salim, D., Tarq Sabar, Z., Sahib Abd, D. and Hasan, A.F. (2025). Changes in the level of lipid profile in diabetes mellitus in samples patients. *Journal of Bioscience and Applied Research.* **11(1):** 331-336.

Mishra, V., Baranwal, V., Mishra, R.K., Sharma, S., Paul, B. and Pandey, A.C. (2020). Immunotoxicological impact and biodistribution assessment of bismuth selenide (Bi2Se3) nanoparticles following intratracheal instillation in mice. *Scientific Reports.* **10(1):** 18032.

Obaid, R.M., Yaseen, F.T. and Mukhlif, M.Y. (2020). Blood cells depletion after chemotherapy in iraqi women with breast cancer. *Indian Journal of Forensic Medicine and Toxicology.* **14(4):** 3379-3382.

Obaid, R.M., Yaseen, F.T. and Salim, A.K. (2020). Correlation between vitamin D3 (cholecalciferol) and thyroid diseases in Iraqi patients. *Annals of Tropical Medicine and Public Health.* **23:** 231-603.

Ohkawa, H., Ohishi, N., Yagi, K. (1979). Assay for lipid peroxides in animal tissues by thiobarbituric acid reaction. *Anal. Biochem.* **95:** 351-358.

Patton, C.J., Crouch, S.R. (1977). Spectrophotometeric and kinetics investigation of the Berthelot reaction for determination of ammonia. *Anal Chem.* **49:** 464-469.

Pereira, B.C.R.L.F., Rosa, L.C., Safi, D.A., Medeiros, M.H.G.D., Curi, R. and Bechara, E.J.H. (1994). Superoxide dismutase, catalase and glutathione peroxidase activities in muscle and lymphoid organs of sedentary and exercise-trained rats. *Physiology and Behavior.* **56(5):** 1095-1099.

Radu, M., Din, I.M., Hermenean, A., Cintezã, O.L., Burlacu, R., Ardelean, A. and Dinischiotu, A. (2015). Exposure to iron oxide nanoparticles coated with phospholipid-based polymeric micelles induces biochemical and histopathological pulmonary changes in mice. *International Journal of Molecular Sciences.* **16(12):** 29417-29435.

Reddy, U.A., Prabhakar, P.V. and Mahboob, M. (2017). Biomarkers of oxidative stress for *in vivo* assessment of toxicological effects of iron oxide nanoparticles. *Saudi Journal of Biological Sciences.* **24(6):** 1172-1180.

Salimi, M., Sarkar, S., Hashemi, M. and Saber, R. (2020). Treatment of breast cancer-bearing BALB/c mice with magnetic hyperthermia using dendrimer functionalized iron-oxide nanoparticles. *Nanomaterials.* **10(11):** 2310.

Sharma, A., Cornejo, C., Mihalic, J., Geyh, A., Bordelon, D.E., Korangath, P. and Ivkov, R. (2018). Physical characterization and *in vivo* organ distribution of coated iron oxide nanoparticles. *Scientific Reports.* **8(1):** 4916.

Saleh, M.M., Sabbah, M.A. and Zedan, Z.K. (2024). Isolation and characterization of three lytic bacteriophages to overcome multidrug-extensive drug-and pandrug-resistant pseudomonas aeruginosa. *PHAGE.* **5(4):** 230-240.

Tate, J.A., Ogden, J.A., Strawbridge, R.R., Pierce, Z.E. and Hoopes, P.J. (2009). Toxicity and biodistribution of activated and non-activated intravenous iron oxide nanoparticles. *In Energy-based Treatment of Tissue and Assessment V SPIE.* **7181:** 211-218.

Velikova, V., Yordanov, I., Edreva, A. (2000). Oxidative stress and some antioxidant systems in acid rain-treated bean plants protective role of exogenous polyamines. *Plant Science.* **151:** 59-66.

Wang, L., Wang, L., Ding, W. and Zhang, F. (2010). Acute toxicity of ferric oxide and zinc oxide nanoparticles in rats. *Journal of Nanoscience and Nanotechnology.* **10(12):** 8617-8624.

Yahya, A., Adil Obaid, W., Mohammed Hameed, O. and Hasan, A.F. (2024). Histopathological and immunohistochemical studies on the effects of silver oxide nanoparticles (AgNPs) on male rats' liver. *Journal of Bioscience and Applied Research.* **10(3):** 392-398.

Yang, L., Kuang, H., Zhang, W., Aguilar, Z.P., Xiong, Y., Lai, W. and Wei, H. (2015). Size dependent biodistribution and toxicokinetics of iron oxide magnetic nanoparticles in mice. *Nanoscale.* **7(2):** 625-636.

Yaseen, T.F., Al-Jumaily, K.M.R. (2025). The impact of interleukin-21 and 23 serum level and gene expression in celiac disease among sample of Iraqi patients. *Asian Journal of Dairy and Food Research.* **44(2):** 234-239. doi: 10.18805/ajdfr.DRF-476.

Yaseen, F.T. and Al-Jumaily, R.M.K. (2024). Evaluation of global DNA methylation, homocysteine and vitamin B12 levels among patients with celiac disease. *Gastroenterology.* **58(4):** 258-263.

Ying, H., Ruan, Y., Zeng, Z., Bai, Y., Xu, J. and Chen, S. (2022). Iron oxide nanoparticles size-dependently activate mouse primary macrophages *via* oxidative stress and endoplasmic reticulum stress. *International Immuno Pharmacology*. **105:** 108533.

Zhang, J., Ring, H.L., Hurley, K.R., Shao, Q., Carlson, C.S., Idiyatullin, D. and Garwood, M. (2017). Quantification and biodistribution of iron oxide nanoparticles in the primary clearance organs of mice using T1 contrast for heating. *Magnetic Resonance in Medicine.* **78(2):** 702-712.

Zedan, Z.K. and AL-Amer, S.H. (2022). The Dysregulation of mir-21 and mir-143 as a clinical marker for cancer stem cells in tissue samples of iraqi male patients with gastrointestinal sarcoma. *Journal of Pharmaceutical Negative Results.* **13(3):** 20.

Zedan, Z.K. and Al-Ameri, S.H.A. (2023). *In vitro* study of primary isolation and culture of adipose-derived stem cells and induction of chondrogenic differentiation. *Archives of Razi Institute.* **78(1):** 125.